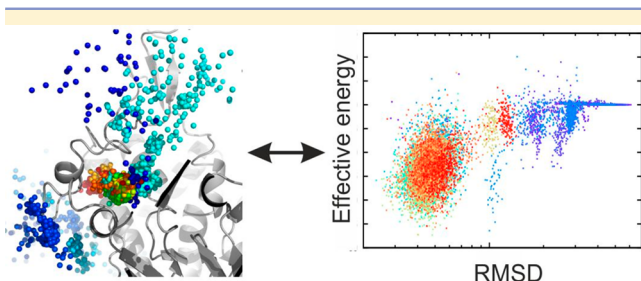


# Binding Region of Alanopine Dehydrogenase Predicted by Unbiased Molecular Dynamics Simulations of Ligand Diffusion

Holger Gohlke,<sup>\*,†</sup> Ulrike Hergert,<sup>‡</sup> Tatjana Meyer,<sup>‡</sup> Daniel Mulnaes,<sup>†</sup> Manfred K. Grieshaber,<sup>‡</sup> Sander H. J. Smits,<sup>‡</sup> and Lutz Schmitt<sup>\*,‡</sup>

<sup>†</sup>Institute for Pharmaceutical and Medicinal Chemistry and <sup>‡</sup>Institute of Biochemistry, Department of Mathematics and Natural Sciences, Heinrich-Heine-University, 40204 Düsseldorf, Germany

## Supporting Information



**ABSTRACT:** Opine dehydrogenases catalyze the reductive condensation of pyruvate with L-amino acids. Biochemical characterization of alanopine dehydrogenase from *Arenicola marina* revealed that this enzyme is highly specific for L-alanine. Unbiased molecular dynamics simulations with a homology model of alanopine dehydrogenase captured the binding of L-alanine diffusing from solvent to a putative binding region near a distinct helix-kink-helix motif. These results and sequence comparisons reveal how mutations and insertions within this motif dictate the L-amino acid specificity.

Unbiased MD simulations of ligand binding have become possible only recently due to advances in the simulation algorithms and hardware. In addition to identifying the binding region of a ligand, they can reveal (un)binding pathways, identify metastable intermediate states, and provide quantitative estimates of binding affinities and on- and off-rates.<sup>1–5</sup> To the best of our knowledge, unbiased MD simulations of ligand binding have not yet been applied for investigating determinants of substrate specificity starting from comparative protein models. Such an application should be widely interesting for other areas of structure-based life sciences as well. In this context, we investigate L-alanine binding to alanopine dehydrogenase of *Arenicola marina* (AlaDHAm)<sup>6</sup> by means of comparative modeling in combination with unbiased molecular dynamics (MD) simulations and a biochemical characterization of AlaDHAm.

AlaDHAm is a member of the family of opine dehydrogenases (OpDHs), which catalyze the reductive condensation of pyruvate with an L-amino acid in the presence of NADH to so-called opines during anaerobic glycolysis.<sup>7</sup> The best characterized enzyme of this family is octopine dehydrogenase (OcDH), which catalyzes the reductive condensation of pyruvate with L-arginine to D-octopine.<sup>8–10</sup> Structures of

OcDH determined by X-ray crystallography in complex with NADH, with NADH and L-arginine as well as with NADH and pyruvate<sup>11</sup> demonstrated that domain I of OcDH binds the cofactor NADH, whereas the main binding site of the amino acid substrate is located in domain II. The binding of L-arginine induces a rotational movement of domain II toward domain I.<sup>11–13</sup> AlaDHAm catalyzes the reductive condensation of pyruvate with L-alanine to alanopine (N-(1-D-carboxylethyl)-L-alanine).<sup>14,15</sup> With lower efficiency also glycine can be used as amino acid precursor, which results in the formation of strombine (N-(carboxymethyl)-D-alanine).<sup>7</sup> In contrast to OcDH, but in agreement with N-(1-D-carboxylethyl)-L-norvaline dehydrogenase (CENDH),<sup>16</sup> AlaDHAm contains a characteristic insertion at position 209 in the helix-kink-helix motif located at the N-terminal part of domain II (AlaDHAm numbering is used throughout this study; Figure S1 in the Supporting Information (SI)). In OpDHs having an N209 insertion, almost exclusively valine is found at position 208 then, whereas in OpDHs lacking N209, aspartate, arginine, lysine, or tyrosine is found at position 208 depending on the respective L-amino acid substrate.<sup>11</sup> CENDH has been crystallized only in the *apo* form, and no structural information is available for AlaDHAm. Thus, the role of sequence positions 208 and 209 in the helix-kink-helix motif in determining the specificity for the L-amino acid substrate in OpDHs has remained elusive.

In order to elucidate this role, first, we biochemically characterized AlaDHAm. Cloning and expression of the gene of AlaDHAm (Uniprot entry: B5D5P2\_AREMA) was performed as described for OcDH from *P. maximus*<sup>10</sup> (see SI for details). The final preparation contained a single homogeneous protein of approximately 45 kDa (SI Figure S2), in agreement with the sequence-based calculated mass and the molecular mass estimated by size-exclusion chromatography using standard proteins (results not shown). The AlaDHAm followed standard Michaelis–Menten kinetics for the substrates used (Figure 1 and Table 1). Substrate inhibition was observed for L-alanine as well glycine, a feature observed for many other OpDHs.<sup>17</sup> For L-alanine, a  $K_m$  of  $14.8 \pm 2.1$  mM and a  $V_{max}$  of  $1513.0 \pm 144.5$  U/mg was found (Table 1). Thus, AlaDHAm is highly active, in contrast to other AlaDH characterized:<sup>18</sup> The AlaDH from *M. sanguinea* displays an almost 20-fold reduced catalytic efficiency ( $k_{cat}$  for AlaDH is 1084.6 and  $51.70\text{ s}^{-1}$  for *A. marina* and *M. sanguinea*, respectively). Furthermore, AlaDHAm displays a

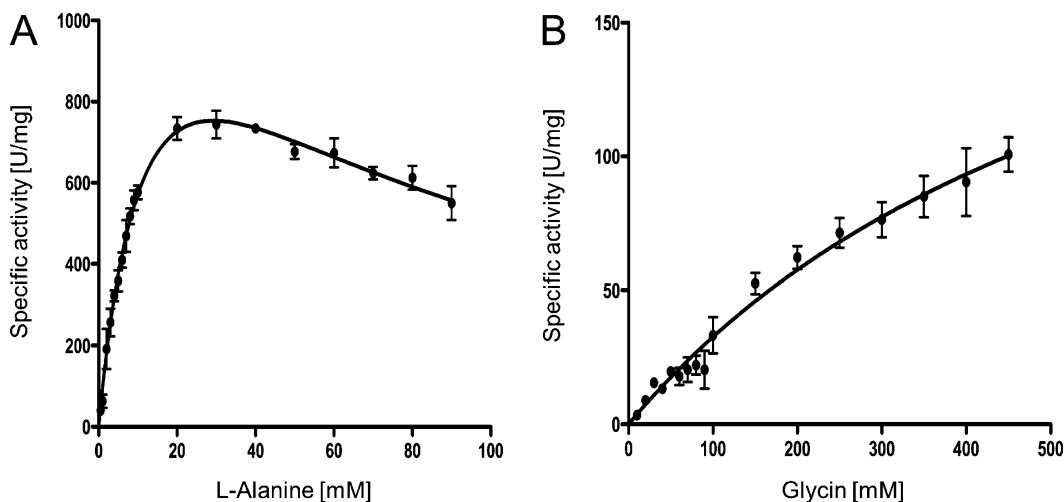


**Figure 1.** Michaelis–Menten kinetics of the alanopine reaction. Plotted is the specific activity of the AlaDHAm against increasing amounts of (A) L-alanine and (B) glycine. The enzymatic activity of AlaDHAm was measured spectrophotometrically at 25 °C following the decrease in absorbance at 340 nm. Standard assays were carried out using 3 mM pyruvate, 0.16 mM NADH in 50 mM triethanolamine buffer pH 7.0. The reaction was started by the addition of L-alanine or glycine. Activities were calculated using a specific absorbance coefficient  $\epsilon = 6.31 \text{ mM}^{-1} \text{ cm}^{-1}$  for NADH. One unit is defined as the amount of enzyme catalyzing the oxidation of 1 μmol NADH per minute.

**Table 1. Kinetic Parameters for the Forward Reaction (NADH Oxidation) Catalyzed by AlaDHAm<sup>a</sup>**

| substrate   | L-alanine          | glycine          |
|---|--------------------|------------------|
| $K_m [\text{mmol L}^{-1}]$                                | $14.8 \pm 2.1$     | $655.1 \pm 45.2$ |
| $V_m [\text{U mg}^{-1}]$                                  | $1513.0 \pm 144.5$ | $246.1 \pm 32.1$ |
| $K_i [\text{mmol L}^{-1}]$                                | $58.0 \pm 10.5$    | b                |
| $k_{\text{cat}} [\text{s}^{-1}]$                          | $1084.6 \pm 78.1$  | $176.4 \pm 24.1$ |
| catalytic efficiency [ $\text{mol}^{-1} \text{ s}^{-1}$ ] | $7.3 \times 10^4$  | b                |

<sup>a</sup>For the determination of the kinetic constants, the initial velocities at different substrate concentrations of L-alanine or glycine were recorded spectrophotometrically at 340 nm. Kinetic parameters were obtained using nonlinear least-squares analysis of the data fitted to the Michaelis–Menten rate equation ( $v = V_{\max}[S]/K_m + [S]$ ) or the Michaelis–Menten equation corrected for uncompetitive substrate inhibition ( $v = V_{\max}[S]/K_m + [S](1 + [S]/K_i)$ ) where  $v$  is the velocity,  $V_{\max}$  is the maximum velocity,  $[S]$  is the substrate concentration,  $K_m$  is the Michaelis constant, and  $K_i$  is the inhibition constant, using the enzyme kinetic module 2.0 of Sigma-plot 9.0 (Systat Software, Erkrath, Germany).

bNot determined.

high specificity toward L-alanine: When glycine was used as a substrate, activity dropped at least 3- to 4-fold with a significantly higher  $K_m$  value suggesting a significantly lower affinity (Table 1), whereas for other small amino acids tested, e.g. L-serine, L-threonine, L-cysteine, or L-valine, no or only negligible activities were found (data not shown). In contrast, the AlaDH from *M. sanguinea* displayed a broader substrate specificity allowing also other small amino acids to form the corresponding opine.<sup>18</sup> This suggests that the binding site for the amino acid has been optimized in AlaDHAm to preferentially bind L-alanine with high efficiency.

In order to structurally elucidate the binding region of L-alanine in AlaDHAm, a model of the protein was generated by comparative modeling using the in-house workflow TopModel (D. Mulnaes and H. Gohlke, unpublished results), which is based on the Modeler program<sup>19</sup> (see SI for details). Pursuing a multitemplate modeling strategy, a pBLAST<sup>20</sup> search on the Protein Data Base<sup>21</sup> revealed three suitable template structures, two of which are OcDHs bound to NADH and either L-arginine (PDB code 3C7C)<sup>11</sup> or agmatine (3IQD).<sup>12</sup> The third

template was CENDH (1BG6).<sup>16</sup> The sequence identities of AlaDHAm with OcDH and CENDH are 46% and 20%, respectively.

A multiple sequence alignment using structural information from the templates revealed a high degree of residue conservation for sequence positions in the vicinity of the substrate-binding region identified in OcDH and respective sequence positions in AlaDHAm (SI Figure S1). In particular, E141 of domain I and W279 of domain II are conserved in OcDHs and are present in AlaDHAm, too. Thus, the substrate specificity toward L-alanine of AlaDHAm cannot be mediated by these amino acids. Y208 of OcDH from *P. maximus* located in the kink of the helix-kink-helix motif is the only amino acid involved in substrate binding that differs between the OcDHs. In addition, in AlaDHAm, N209 is inserted. As position 209 is also located in the kink, N209 can be accommodated in the model structure of AlaDHAm without disturbing the overall structure (SI Figure S3A; see the Homology modeling section in the SI for an evaluation of the structural quality of the model). An overlay of the L-arginine bound OcDH structure with the AlaDHAm model indicated that the inserted amino acid would sterically interfere with the binding position of L-arginine (Figure S3B). Accordingly, while for the generation of an AlaDHAm/NADH/L-alanine model the coordinates of NADH could be copied from the OcDH/NADH/L-arginine complex structure without steric clashes, a geometry optimization was required to reduce steric clashes of the L-alanine substrate initially placed at the position of the backbone of the arginine substrate (see Supporting Information for details). The optimized binding pose of L-alanine is shifted by ~3 Å with respect to the starting location (Figure S3B).

To further refine the AlaDHAm/NADH/L-alanine complex structure, the structure was subjected to three independent molecular dynamics (MD) simulations in explicit solvent of 200 ns length each (see Supporting Information for details on the protocols of the MD simulation). Overall, only moderate deviations of the AlaDHAm structures from the starting structure were observed (root mean-square deviations (rmsd) of the  $C_\alpha$  atoms in all trajectories between 2.5 and 4 Å, in rare cases also up to 4.5 Å; SI Figure S4A and B), which are

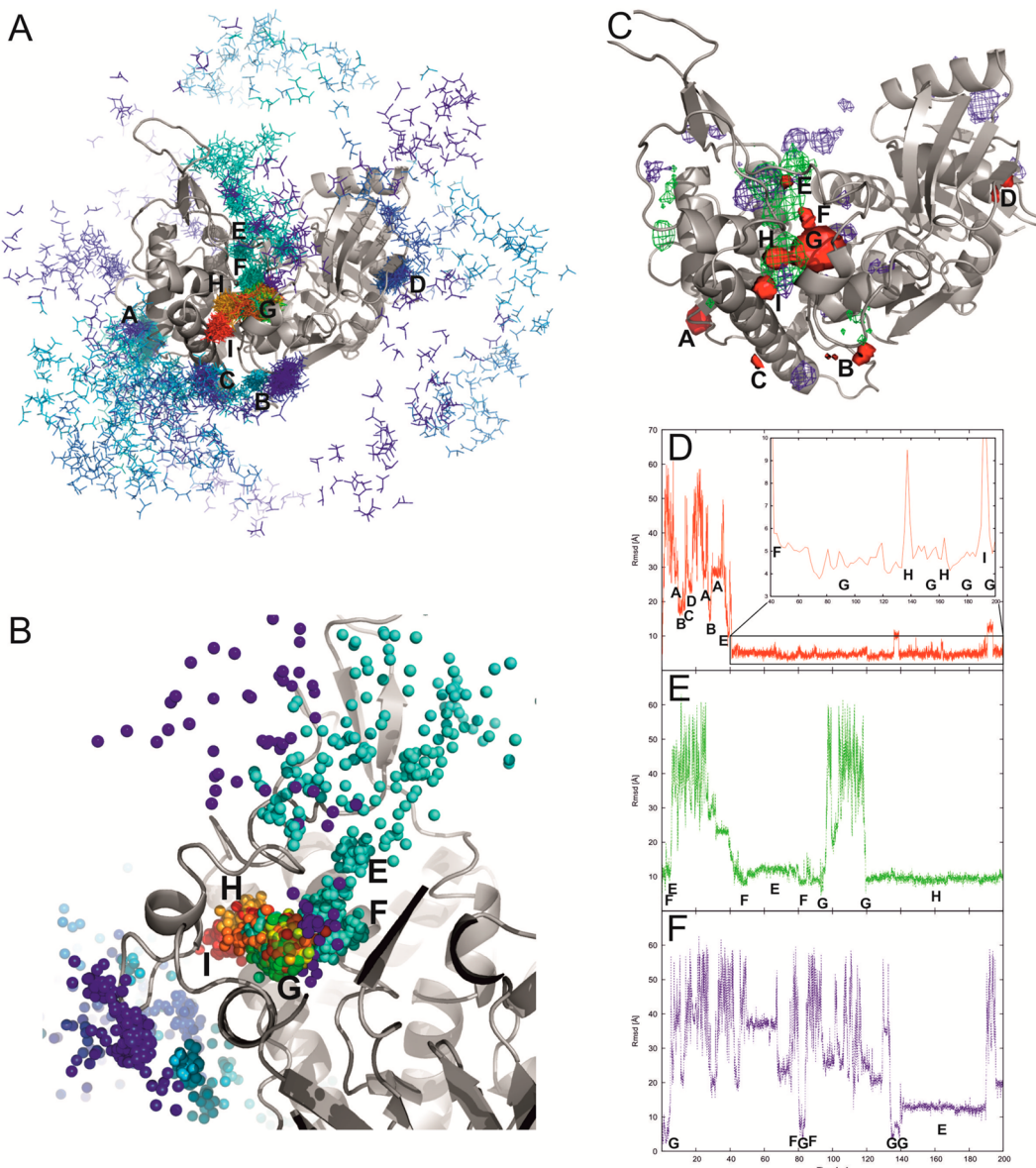


**Figure 2.** Unbiased MD simulations of L-alanine diffusion. (A–F) Black letters indicate regions of high density of L-alanine during the MD simulation 1 as identified in panel C. Region G is the predicted binding region. (A) Traces of L-alanine extracted from the trajectory 1 generated by MD simulations of 200 ns length of the AlaDHAm/NADH/L-alanine system in explicit water (see Supporting Information for details); L-alanine reaches the predicted binding region after  $\sim$ 40 ns (see panel D). The time evolution of the MD simulation is color coded from blue (0 ns) to red (200 ns). For clarity, only a conformation closest to the average conformation of AlaDHAm is shown (gray cartoon). (B) Close-up view of the predicted binding region shown in panel A with the trace of C<sub>α</sub> atoms of L-alanine extracted from trajectory 1 shown as spheres. See panel A regarding the color coding. (C) Overlay of density maps extracted from trajectories 1 (red isocontour surface), 2 (green isocontour mesh), and 3 (blue isocontour mesh) showing the frequency of interactions of L-alanine on the surface of AlaDHAm; the contour level is 3 sigma. Regions of high density identified from trajectory 1 are labeled with black letters. The protein conformation is as in panel A. (D–F) Root mean square deviations (rmsds) of the L-alanine atoms during the course of the MD simulations 1 (panel D), 2 (panel E), and 3 (panel F) with respect to the modeled starting structure (see SI Figure S3) after superimposing AlaDHAm based on its C<sub>α</sub> atoms.

comparable to those observed when MD simulations of 100 ns length are started from one of the crystal structures used as a template (PDB ID 3C7C; rmsd = 1.5–3.5 Å; data not shown). NADH remained at its binding position in all three simulations (Figure S4). However, despite a careful thermalization of the complex structures, the ligand, L-alanine, left the initial binding region after at most 5 ns in all three simulations and escaped into the solvent (rmsd up to 60 Å; Figure 2A–F). Yet, L-alanine spontaneously returned to this region after 40 ns in MD simulation 1 (Figure 2A, B, and D; the binding region is marked with a “G”) and remained bound for almost all of the

remaining simulation time. Similar returns are observed in MD simulation 2 (after 95 and 120 ns) and 3 (after 82 and around 137 ns) with residence times of L-alanine of at most 6 ns (Figure 2E and F). Such short residence times do not contradict expectations arising from the knowledge of the very weak binding affinity observed for L-alanine to AlaDHAm ( $K_i = 58.0 \pm 10$  mM; Table 1). These MD results are remarkable for three reasons: (I) initially, the ligand completely escapes to the solvent (see the trace of L-alanine in MD simulation 1 in Figure 2A) and diffuses there for at least 40 ns before rebinding such that the rebinding should not be

influenced by the starting position; (II) the observed binding events occurred from unbiased MD simulations, i.e. no prior knowledge of the binding region was applied during the MD simulations; (III) it is reassuring that in all three independent MD simulations L-alanine does bind again. In all, this makes our MD simulations one of the few examples<sup>1–5</sup> known to date that capture binding of a ligand diffusing from solvent to the bound state.

In order to provide quantitative estimates of the binding thermodynamics and kinetics<sup>4</sup> substantially more observed unbinding and binding events would have been required. In particular, sampling of the unbound state is not converged after 200 ns of simulation time as demonstrated by nonoverlapping regions of highest frequency of L-alanine interactions on the outer surface of AlaDHAm in MD simulations 1–3 (Figure 2C). Still, the simulations provide suggestions for energetically favorable interaction “hot spots” on the protein’s outside, as exemplarily shown for L-alanine “hopping” between regions A–D in MD simulation 1 (Figure 2A, C, and D). In contrast, all three MD simulations yield overlapping densities of the frequency of L-alanine interactions with AlaDHAm when L-alanine approaches the bound state, i.e., for regions E, F, G, and H (Figure 2B and C). When mapped onto the MD trajectories, these findings suggest that L-alanine consistently unbinds from (and binds to) region G via regions F and E (Figure 2D–F). The effective energy of binding  $\Delta G_{\text{effective}}$  (i.e., the sum of gas-phase and solvation free energy) computed along MD trajectory 1 by the MM-GBSA method (see Supporting Information for details)<sup>22</sup> corroborates this view, which shows a global effective energy minimum corresponding to L-alanine binding to region G accompanied by several local minima corresponding to L-alanine in non-native poses (the most pronounced of which refers to region E) (Figure 3A; SI Figure SSA). In total, a funnel-shaped landscape<sup>23–25</sup> of the binding effective energy emerges, which is similar to landscapes of the binding effective energy observed for the binding of kinase inhibitors to the Src kinase.<sup>1</sup> Contributions due to the changes in the configurational entropy of the solute molecules upon binding are not considered in the effective energy calculations. Considering that bound L-alanine shows a considerable amount of residual motions as judged from the observation of configurational fluctuations of L-alanine of ~3 Å in region G (Figures 2D and 3A), adverse contributions to binding due to changes in the configurational entropy are expected to be small (see SI Supplemental Results for an estimate). Thus, the overall shape of a landscape of the free energy of binding should not differ qualitatively from our landscape. Finally, from these calculations, three energetically most favorable and non-distinguishable L-alanine positions ( $\Delta G_{\text{effective}} = -27.34$ ,  $-27.38$ ,  $-27.25$  kcal mol<sup>-1</sup>) are identified which all reside in region G (Figure 3A; Figure SSA). When computing the effective energy of binding for MD trajectories 2 and 3,  $\Delta G_{\text{effective}} = -16.73$  and  $-13.4$  kcal mol<sup>-1</sup> are found for L-alanine positions in region G, respectively (SI Figure S6); these values are among the most favorable effective energies computed in both cases. Global minima are found at  $\Delta G_{\text{effective}} = -22.23$  and  $-24.68$  kcal mol<sup>-1</sup> for these trajectories, respectively; the corresponding L-alanine positions belong to regions H and E (Figures S6 and 2E and F). The time series of  $\Delta G_{\text{effective}}$  values identify these cases as singletons, however, suggesting that the energy wells associated with these minima are narrow and that, accordingly, adverse contributions to binding due to changes in the configurational entropy should

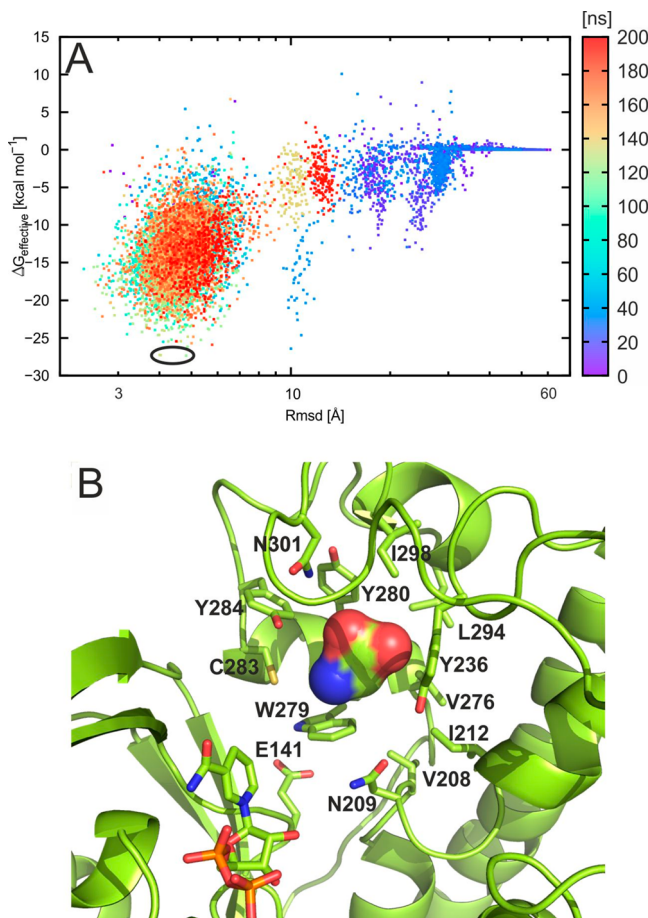


**Figure 3.** Effective binding energy calculations and predicted binding region. (A) Effective energies (i.e., the sum of gas-phase and solvation free energies) of L-alanine binding to AlaDHAm calculated by the MM-GBSA approach (see Supporting Information for details) along the trajectory 1 as a function of the L-alanine rmsd with respect to the starting structure. The time evolution along the trajectory is color coded from blue (0 ns) to red (200 ns) (see also color scale). The black circle indicates the three most favorable and energetically indistinguishable AlaDHAm/L-alanine configurations belonging to region G depicted in Figure 2, panels A–D (see also SI Figure S5). A second minimum at ~10 Å rmsd refers to binding in region E. (B) Close-up view of the binding region with one of the three most favorable and energetically indistinguishable AlaDHAm/L-alanine configurations (see Figure S5B for the full structure) obtained from MD simulation 1. The bound L-alanine is depicted by a surface representation to indicate its residual configurational fluctuations of ~3 Å. NADH is depicted as sticks as are residues surrounding the binding region and/or involved in enzymatic function. The side chain of Y304 has been omitted for clarity. Label numbers refer to the AlaDHAm sequence.

be pronounced (Figure S6). Furthermore, these global minima are at least 2.5 kcal mol<sup>-1</sup> higher than those found in MD simulation 1. Thus, in addition to showing the most favorable effective energy of binding found in all MM-GBSA calculations, region G is also most frequently populated across all three MD simulations. These two independent results strongly suggest that region G is the substrate-binding region of AlaDHAm (Figures 3B and SI Figure S5B and C).

Figure 3B reveals that L-alanine is accommodated in a pocket mainly formed by residues Y236, V276, W279, Y280, Y284, L294, N301, and Y304 of domain II, five of which are strictly conserved across OcDH, CENDH, and AlaDHAm (SI Figure

S1). L-Alanine sits with its amino moiety “above” W279, allowing for favorable cation- $\pi$  interactions, thereby pointing with its amino moiety toward a putative binding region of pyruvate; W279 itself is stabilized by weak hydrogen bond interactions with E141 of domain I (occupancy along the trajectory: 16%). E141 and W279 both have been found to be involved in L-arginine binding in OcDH, too.<sup>7</sup> However, in OcDH, the guanidinium moiety of arginine is placed “below” W279 (SI Figure S3); this position is sterically precluded for L-alanine in AlaDHAm by the inserted N209, however. Thus, sequence position 209 is decisive in determining the substrate specificity of AlaDHAm. In OcDH, which lacks position 209, this role is taken over by Y208, which generates a large binding site for the L-arginine side chain.<sup>11</sup> Accordingly, in other OpDHs lacking N209, aspartate, arginine, lysine, or tyrosine are found at position 208 depending on the respective amino acid substrate, while almost exclusively valine is found at this position in OpDHs that do have an N209 insertion.<sup>11</sup>

The carboxylate moiety of L-alanine is surrounded by the polar groups of Y280, Y284, N301, and Y304. However, in neither case are strong hydrogen bonds formed as judged from the distances (3.5–4.5 Å); this is in line with the observation of residual mobility of L-alanine when bound to region G (see above). Finally, C<sub>β</sub> of L-alanine points to a wall of aromatic and aliphatic carbons in close proximity. This may explain why larger amino acids such as L-cysteine, L-serine, L-threonine, or L-valine cannot bind to AlaDHAm (see above). In turn, glycine binding may lack the hydrophobic interactions formed by the methyl group of L-alanine, which may explain why the K<sub>m</sub> is ~50-fold higher for glycine than for L-alanine (Table 1).

The binding of L-alanine is accompanied by a rotation of domain II toward the NADH binding domain (domain I; SI Figure S7A). After superimpositioning domain I, this results in an rmsd of the C<sub>α</sub> atoms of domain II of ~3.7 Å with respect to the starting structure. A similar closing movement has been observed when L-arginine binds to an OcDH/NADH complex<sup>11–13</sup> and an even more pronounced closing after pyruvate binding to OcDH/NADH.<sup>7</sup> A bound pyruvate together with the additional closing movement can be expected to restrict the residual mobility observed for L-alanine when bound to region G (see above), which may otherwise hamper an efficient catalysis.

The closing movement of domain II also leads to an enclosed binding region of L-alanine (SI Figure S7B). This together with the (un)binding pathway of L-alanine toward (from) there via the regions E and F (Figure 2A–F) can also provide an explanation at an atomic level as to the observed substrate inhibition of AlaDHAm. Assuming that after the enzymatic reaction alanopine needs to escape the binding region on the same pathway as L-alanine accesses it, this escape will be the more hampered the more L-alanine occupies the energetically favorable (Figures 3A and SSA) regions E and F. The assumption of the same access and escape pathways seems to be justified particularly for the transition between regions F and G, given the narrow, gorge-like character of that region (SI Figure S7B). This narrowness has also been implicated<sup>7</sup> as the reason for the observed binding of substrates to OcDH in a sequential, ordered manner (first L-arginine, then pyruvate).<sup>12,13</sup> Capturing AlaDHAm in an alanopine bound state that way would result in a decrease of the enzymatic reaction velocity that becomes more pronounced with increasing L-alanine concentration.

In summary, we presented an initial biochemical characterization of AlaDHAm, which catalyzes the reductive condensation of L-alanine with pyruvate to alanopine. AlaDHAm displays a high catalytic efficiency and substrate specificity, although it is prone to substrate inhibition. Unbiased MD simulations captured the binding of L-alanine diffusing from solvent to the putative binding region. This binding region is located at the helix-kink-helix motif, as observed for binding of L-arginine to OcDH from *P. maximus*. At the same time, the observed binding of L-alanine provides an explanation for the role of amino acids 208 and 209 in substrate specificity, the only amino acids within the binding region that differ between OpDHs with different substrates. Finally, the presence of energetically favorable non-native ligand binding states in the vicinity of the binding region can provide an explanation for the substrate inhibition of AlaDHAm.

## ■ ASSOCIATED CONTENT

### ● Supporting Information

Material and methods, results on estimating changes in the configurational entropy upon binding, and figures of the alignment of sequences of AlaDHAm and the three templates, Coomassie stained SDS-PAGE of AlaDHAm from different purification steps, modeled AlaDHAm/NADH/L-alanine starting structure vs OcDH/NADH/L-arginine crystal structure, structural deviations during the MD simulations, effective binding energies and energetically most favorable AlaDHAm/L-alanine configurations, time course of effective energies of binding of L-alanine to AlaDHAm for MD simulations 2 and 3, and movement of domain II of AlaDHAm relative to domain I in the course of L-alanine binding. This material is available free of charge via the Internet at <http://pubs.acs.org>.

## ■ AUTHOR INFORMATION

### Corresponding Authors

\*Phone: +49(0)221-81-13662. E-mail: gohlke@hhu.de (H.G.).

\*Phone: +49(0)221-81-10773. E-mail: lutz.schmitt@hhu.de (L.S.).

### Notes

The authors declare no competing financial interest.

## ■ ACKNOWLEDGMENTS

We gratefully acknowledge support (and training) from the International NRW Research School BioStruct, granted by the Ministry of Innovation, Science and Research of the State North Rhine-Westphalia, the Heinrich-Heine-University of Düsseldorf (HHU), and the Entrepreneur Foundation at the HHU. H.G. is grateful to the initiative “Fit for Excellence” of the HHU for financial support and to the “Zentrum für Informations- und Medientechnologie” (ZIM) at the HHU for providing computational support. Some of this work has been supported by the DFG (grant GR 456/23-1 to M.K.G.).

## ■ ABBREVIATIONS

AlaDH, alanopine dehydrogenase; AlaDHAm, alanopine dehydrogenase from *Arenicola marina*; CENDH, N-(1-D-carboxylethyl)-L-norvaline dehydrogenase; MD, molecular dynamics; MM-GBSA, molecular mechanics generalized Born surface area; OpDH, opine dehydrogenase; OcDH, octopine dehydrogenase; rmsd, root mean-square deviation

## ■ REFERENCES

- (1) Shan, Y. B.; Kim, E. T.; Eastwood, M. P.; Dror, R. O.; Seeliger, M. A.; Shaw, D. E. How Does a Drug Molecule Find Its Target Binding Site? *J. Am. Chem. Soc.* **2011**, *133* (24), 9181–9183.
- (2) Dror, R. O.; Pan, A. C.; Arlow, D. H.; Borhani, D. W.; Maragakis, P.; Shan, Y.; Xu, H.; Shaw, D. E. Pathway and mechanism of drug binding to G-protein-coupled receptors. *Proc. Natl. Acad. Sci. U.S.A.* **2011**, *108* (32), 13118–23.
- (3) Giorgino, T.; Buch, I.; De Fabritiis, G. Visualizing the Induced Binding of SH2-Phosphopeptide. *J. Chem. Theory. Comput.* **2012**, *8* (4), 1171–1175.
- (4) Buch, I.; Giorgino, T.; De Fabritiis, G. Complete reconstruction of an enzyme-inhibitor binding process by molecular dynamics simulations. *Proc. Natl. Acad. Sci. U.S.A.* **2011**, *108* (25), 10184–10189.
- (5) Kruse, A. C.; Hu, J.; Pan, A. C.; Arlow, D. H.; Rosenbaum, D. M.; Rosemond, E.; Green, H. F.; Liu, T.; Chae, P. S.; Dror, R. O.; Shaw, D. E.; Weis, W. I.; Wess, J.; Kobilka, B. K. Structure and dynamics of the M3 muscarinic acetylcholine receptor. *Nature* **2012**, *482* (7386), 552–6.
- (6) Zebe, E.; Schiedeck, D. The lugworm *Arenicola marina*: a model of physiological adaptation to life in intertidal sediments. *Helgoländer Meeresunters* **1996**, *30*, 37–68.
- (7) Grieshaber, M. K.; Hardewig, I.; Kreutzer, U.; Portner, H. O. Physiological and metabolic responses to hypoxia in invertebrates. *Rev. Physiol. Biochem. Pharmacol.* **1994**, *125*, 43–147.
- (8) van Thoai, N.; Huc, C.; Pho, D. B.; Olomucki, A. Octopine dehydrogenase. Purification and catalytic properties. *Biochim. Biophys. Acta* **1969**, *191* (1), 46–57.
- (9) Pho, D. B.; Olomucki, A.; Huc, C.; Thoai, N. V. Spectrophotometric studies of binary and ternary complexes of octopine dehydrogenase. *Biochim. Biophys. Acta* **1970**, *206* (1), 46–53.
- (10) Muller, A.; Janssen, F.; Grieshaber, M. K. Putative reaction mechanism of heterologously expressed octopine dehydrogenase from the great scallop, *Pecten maximus* (L.). *Febs. J.* **2007**, *274* (24), 6329–6339.
- (11) Smits, S. H.; Mueller, A.; Schmitt, L.; Grieshaber, M. K. A structural basis for substrate selectivity and stereoselectivity in octopine dehydrogenase from *Pecten maximus*. *J. Mol. Biol.* **2008**, *381* (1), 200–11.
- (12) Smits, S. H.; Meyer, T.; Mueller, A.; van Os, N.; Stoldt, M.; Willbold, D.; Schmitt, L.; Grieshaber, M. K. Insights into the mechanism of ligand binding to octopine dehydrogenase from *Pecten maximus* by NMR and crystallography. *PLoS One* **2010**, *5* (8), e12312.
- (13) van Os, N.; Smits, S. H. J.; Schmitt, L.; Grieshaber, M. K. Control of D-octopine formation in scallop adductor muscle as revealed through thermodynamic studies of octopine dehydrogenase. *J. Exp. Biol.* **2012**, *215* (9), 1515–1522.
- (14) Siegmund, B.; Grieshaber, M.; Reitze, M.; Zebe, E. Alanopine and Strombine Are End Products of Anaerobic Glycolysis in the Lugworm, *Arenicola-Marina*-L (Annelida, Polychaeta). *Comp. Biochem. Physiol. B: Biochem. Mol. Biol.* **1985**, *82* (2), 337–345.
- (15) Siegmund, B.; Grieshaber, M. K. Determination of meso-alanopine and D-strombine by high pressure liquid chromatography in extracts from marine invertebrates. *Hoppe Seylers Z. Physiol. Chem.* **1983**, *364* (7), 807–12.
- (16) Britton, K. L.; Asano, Y.; Rice, D. W. Crystal structure and active site location of N-(1-D-carboxylethyl)-L-norvaline dehydrogenase. *Nat. Struct. Biol.* **1998**, *5* (7), 593–601.
- (17) Gade, G.; Grieshaber, M. K. Pyruvate Reductases Catalyze the Formation of Lactate and Opines in Anaerobic Invertebrates. *Comp. Biochem. Physiol. B: Biochem. Mol. Biol.* **1986**, *83* (2), 255–272.
- (18) Endo, N.; Kan-No, N.; Nagahisa, E. Purification, characterization, and cDNA cloning of opine dehydrogenases from the polychaete rockworm *Marpissa sanguinea*. *Comp. Biochem. Physiol. B: Biochem. Mol. Biol.* **2007**, *147* (2), 293–307.
- (19) Sali, A.; Blundell, T. L. Comparative protein modelling by satisfaction of spatial restraints. *J. Mol. Biol.* **1993**, *234* (3), 779–815.
- (20) Altschul, S. F.; Gish, W.; Miller, W.; Myers, E. W.; Lipman, D. J. Basic Local Alignment Search Tool. *J. Mol. Biol.* **1990**, *215* (3), 403–410.
- (21) Berman, H. M.; Westbrook, J.; Feng, Z.; Gilliland, G.; Bhat, T. N.; Weissig, H.; Shindyalov, I. N.; Bourne, P. E. The Protein Data Bank. *Nucleic Acids Res.* **2000**, *28* (1), 235–242.
- (22) Gohlke, H.; Kiel, C.; Case, D. A. Insights into protein-protein binding by free energy calculation and free energy decomposition for the Ras-Raf and Ras-RalGDS complexes. *J. Mol. Biol.* **2003**, *330*, 891–913.
- (23) Bryngelson, J. D.; Onuchic, J. N.; Soccia, N. D.; Wolynes, P. G. Funnels, pathways, and the energy landscape of protein folding: a synthesis. *Proteins* **1995**, *21* (3), 167–195.
- (24) Wang, J.; Verkhivker, G. M. Energy landscape theory, funnels, specificity, and optimal criterion of biomolecular binding. *Phys. Rev. Lett.* **2003**, *90* (18), 188101.
- (25) Tsai, C.-J.; Kumar, S.; Ma, B.; Nussinov, R. Folding funnels, binding funnels, and protein function. *Protein Sci.* **1999**, *8*, 1181–1190.